Immobilization of Active α-Chymotrypsin on RF-Plasma-Functionalized Polymer Surfaces

R. GANAPATHY,[1] S. MANOLACHE,[1] M. SARMADI,[2] W. J. SIMONSICK, JR.,[3] F. DENES[1]

[1] Center for Plasma-Aided Manufacturing, University of Wisconsin-Madison, Madison, WI 53706

[2] School of Human Ecology, University of Wisconsin-Madison, Madison, WI 53706

[3] Du Pont Automotive, Marshall R & D Laboratory, Philadelphia, PA, 19146

Received 4 April 1999; accepted 8 October 1999

ABSTRACT: Various polymeric surfaces (polyester, polyethylene, polystyrene) were functionalized under oxygen and dichlorosilane-RF-cold-plasma environments and were employed as substrates for further in situ derivatization reactions and immobilization of α-Chymotrypsin. The nature and morphology of the derivatized substrates and the substrates with immobilized enzymes were analyzed using survey and high-resolution X-ray photoelectron spectroscopy, attenuated total reflectance-fourier transform infrared (ATR-FTIR), laser desorption fourier transform ion cyclotron resonance mass spectrometry, chemical derivatization, and atomic force microscopy (AFM) techniques. It was demonstrated that the tacticity of the polystyrene substrate did not notably influence the activity of the immobilized enzyme, however, spacer molecules intercalated between the polymeric substrates (e.g., polyethylene) and the enzyme significantly increased the enzyme activity (comparable with that of the free enzyme). Computer-aided conformational modeling of the substrate-spacer systems indicated that the longer the spacer chain, the greater the mobility of the enzyme. It is suggested that the greater mobility of the enzyme molecules is responsible for the enhanced activity. It has also been shown that the stability of the immobilized enzyme systems was good; they retained their activity during several washing/assay cycles. © 2000 John Wiley & Sons, Inc. J Appl Polym Sci 78: 1783–1796, 2000

Key words: plasma functionalized surface; α-Chymotrypsin; enzyme immobilization; spacer; surface morphology

INTRODUCTION

The advantages of using enzymes in chemical synthesis are related to their very high specificity (regio- and stereo-specificity) and versatility, mild reaction conditions (close to room temperatures and to pH neutral media), and to their high reaction rates.[1–3] However, due to the poor recovery yields and reusability of free enzymes much attention has been paid in the last years to the development of efficient enzyme immobilization processes. Most biologically active in vivo species, such as enzymes and antibodies, function in heterogeneous media. These environments are difficult to reproduce in vitro for industrial utilization. Immobilized enzyme systems are useful experimental and theoretical research purposes for understanding the mechanisms of in vivo, biocatalyzed reactions, and offer solutions for use in batch-type reactions, where there is poor adaptability to various technological designs and recovery of the enzymes is difficult.

Correspondence to: F. Denes.

Journal of Applied Polymer Science, Vol. 78, 1783–1796 (2000)

The molecular recognition ability and activity of enzymes (polypeptide molecules) are based on their complex three-dimensional structures containing sterically exposed, specific functionalities. The polypeptide chains are folded into one or several discrete units (domains), which represent the basic functional and three-dimensional structural entities. The cores of domains are composed of a combination of motifs that are combinations of secondary structure elements with a specific geometric arrangement. The molecular-structure-driven chain-folding mechanisms generate three-dimensional enzyme structures with protein molecules orienting their hydrophobic side chains toward the interior and exposing a hydrophilic surface. The —C(R)—CO—NH— based main chain is also organized into a secondary structure to neutralize its polar components through hydrogen bonds. These structural characteristics are extremely important and they make the enzyme molecules very sensitive to the morphological and functional characteristics of the potential immobilizing substrates. High surface concentrations of enzyme-anchoring functionalities can result for instance, in excessive enzyme densities or multipoint connections that can "neutralize" the active sites or can alter the three-dimensional morphologies of the enzyme molecules through their mutual interaction and their interaction with the substrate surfaces. These are just a few of the factors that may be responsible for the significantly lower activities of immobilized-enzymes in comparison to the activities of free enzyme molecules. Rough substrate surface topographies or stereoregular surfaces (e.g., isotactic or syndiotactic polymers) might also influence, in a positive or negative way, the specific activities. Morphologically ordered surfaces might induce changes of the stereoregular shapes of protein molecules. Recently it has been found that enzymes can adopt more than one functional conformation other than its lowest potential energy state.[4] Consequently, one of the potential solutions for achieving enhanced immobilized enzyme activities, comparable to that of the free enzymes, would be to intercalate selected length and densities of spacer molecules between the substrate and the enzyme molecules during the immobilization reaction processes.[5–9]

In this contribution the influence of the chemical and stereoregular nature of the polymeric substrates, and the length of enzyme-immobilizing spacer molecules[10–12] on the activity of α-Chymotrypsin (AC) immobilized on plasma functionalized polymer surfaces is discussed.

EXPERIMENTAL

Materials and Methods

High-purity argon (Ar) and oxygen was purchased from Liquid Carbonic (Chicago, IL). 1,3 Propylenediamine (99+%) (PD), hexafluoro 1,3 propylenediamine (HFPD), hexafluoroglutaric anhydride (97%) (HFGA), pentafluoropropionic anhydride (99+%) (PFPA), pentafluorophenyl hydrazine (PFPH), and pentafluorophenyl bezaldehyde (PFB) were supplied by Aldrich Co. (Milwaukee, WI). Hexafluoroglutaril chloride (HFGCl) was purchased from Rare Chemical Co. (Milwaukee, WI). All reagents and the technique used for immobilizing AC, and the assay for monitoring the enzyme activity were described earlier.[13] Dichlorosilane (DS) was supplied by Gelest Inc. (Tullytown, PA) (lecture bottle) and it was used as received. Aldrich, atactic (Mw: 400,000) (APS) and isotactic (90%, Mw: 400,000) (IPS) polystyrene substrates (discs of 4 cm diameter and thickness of 1 mm) were prepared using hot pressing technique (temperature of the die: 100°C; pressure: 1 ton/cm^2; vacuum environment; the discs were removed after cooling the die to room temperature). Additive-free polyethylene (PE) films (W.R. Grace Co., Columbia, MD) were used as received. APS, IPS, and PE film samples were acetone extracted then washed with water and dried under vacuum oven conditions. Comparative survey and high-resolution X-ray photoelectron spectroscopy (ESCA) evaluations indicated that the samples do not contain detectable amounts of additives on their surfaces. Accordingly all plasma treatment processes were carried out on samples as received.

Derivatization of carbonyl groups were performed in liquid media.[14] The polymer samples (5 cm^2) were immersed for 2 hours at 25°C, into solutions containing 150 mg PFPH and 1 drop of concentrated HCL in 15 mL 95% ethanol. The substrates were then washed with 100% ethanol and extracted with ether. Primary amine functionalities were labeled in situ gas phase reaction using PFB. Over the freshly functionalized polymeric substrates PFB was distilled and the samples were kept under 1000 mT vapor pressure for 20 min. Vacuum dried samples were used for ESCA evaluations.

Covalent attachment of spacer molecular chains were performed using direct, one-stage, and three-stage reactions. Direct immobilization of AC was performed involving plasma-generated

C═O functionalities. During the one-stage reaction HFGA vapors were introduced (in situ) over DS-plasma functionalized polymer surfaces under vacuum (vapor pressure of HFGA: 1000 mT, reaction time: 20 min; after the reaction was completed the reactor was vacuumed to basic-pressure level). The three-step process was completed by introducing, for instance, over DS-plasma functionalized polymer surfaces HFGA, PD, and HFGCl, consecutively. All sequences were performed at 1000 mT pressure, 20 min reaction time, and by creating base pressure conditions between the consecutive steps.

Evaluation of the relative surface atomic compositions of plasma-modified, derivatized, and enzyme-attached samples were carried out using a Perkin Elmer Physical Electronics 0 5400 small-area ESCA system; Mg source; 15 kV; 300 W; pass energy: 89.45 eV; angle: 45°. Carbon (C1s), oxygen (O1s), nitrogen (N1s), and fluorine (F1s) atomic compositions were evaluated and the binding energy values of the nonequivalent positions of carbon linkages were analyzed. In order to correct surface-charge-origin binding energy shifts calibrations were performed based on the well known C1s peak.

Differential attenuated total reflectance Fourier-transform infrared spectroscopy (ATR-FTIR) was used to identify AC-related chemical linkages on plasma functionalized and enzyme-immobilized polymer surfaces. An ATI-Mattson, Research Series IR instrument was used that was provided with a GRASEBY-Special Benchmark Series ATR in-compartment P/N/ 11160 unit. All FTIR evaluations were performed under nitrogen blanket generated from a flow-controlled liquid nitrogen tank. Data were collected in the 600–4000 cm^{-1} wavenumber region with 250 scans for each sample, with a resolution of 0.4 cm^{-1}. The differential spectra resulted from the subtraction of reference spectra (ATR spectra of surface-functionalized polymers) from the immobilized enzyme-coated polymer ATR spectra were also recorded.

The presence of covalently attached AC on PE substrates was also monitored using laser desorption Fourier transform ion cyclotron resonance mass spectrometry (LD-FT/ICR/MS). A Finnigan FT/MS Newstar system (Madison, WI) operating at 3.0 tesla with the standard dual-trap configuration as previously reported[15] was used in all studies. Experimental control and data interpretation were accomplished by use of Odyssey software running on Sun Microsystem (Mountain View, CA) computer station. The modified samples placed on the sample-holder discs were positioned, with the aid of an automatic insertion probe, approximately 3 mm away from the source trap plate of the ICR cell. The source pressure was less than 3.0×10^{-7} torr (uncorrected ion gauge reading) for all mass evaluations. A Tachisto CO_2 (Needham, MA) laser beam (λ = 10.6 μm, power 10^6–10^8 watts/cm^2, pulse width = 40–80 ns) was fired at the sample-disc producing a spot size of approximately 1 mm^2. The desorbed neutral materials were allowed to drift into the cell for 4 ms and subsequently ionized with a 70 eV electron beam. The source trap plate was set 2.0 V and the back trap plate (conductance limit) was held at 2.0 V (64 K data points). After 2.0 s delay ions were excited by use of linear sweep excitation prior to detection. One zero fill was performed prior to Fourier transformation.

Plasma-induced modifications of surface morphologies of polymer substrates and the new topographies generated as a result of enzyme attachments were evidenced by atomic force microscopy (Digital Instrument Nanoscope III AFM; experimental conditions: scan rate: 2.654 Hz; sampling number: 512) using drycell approach under air environment.

Conformational modeling of spacer molecules (optimizing models, conformational searching, and calculating single point energies for molecules) has been performed using computational tools provided by Chem3D Pro (Version 4, CambridgeSoft, Cambridge, MA, USA), based on molecular mechanics. Global minimum-, as well as, all-conformations that contribute significantly to the experimental properties, were computed using Conformer (Princeton Simulations, New Brunswick, NJ, USA). Conformer uses directly the Chem3D—MM2 force field.

The reproducibility of all plasma-induced modifications and enzyme immobilization reactions were tested by running at least six identical plasma and immobilization procedures, for each specific functionalization reaction. Enzyme-activity assay tests were run in the 0–20 min interval, and the enzyme activity was also tested by reusing thoroughly washed, enzyme-immobilized substrates for as many as five cycles.

All O_2- and DS-plasma functionalization reactions were carried out in a capacitively coupled, parallel-plate (disc-shaped electrodes, diameter: 20 cm; gap between the electrodes, 3 cm; lower electrode, grounded; upper electrode, connected to the 40 kHz RF-power supply) cylindrical, stainless steel reactor, described earlier.[14] In a typical experiment, after the specific polymeric substrate was intro-

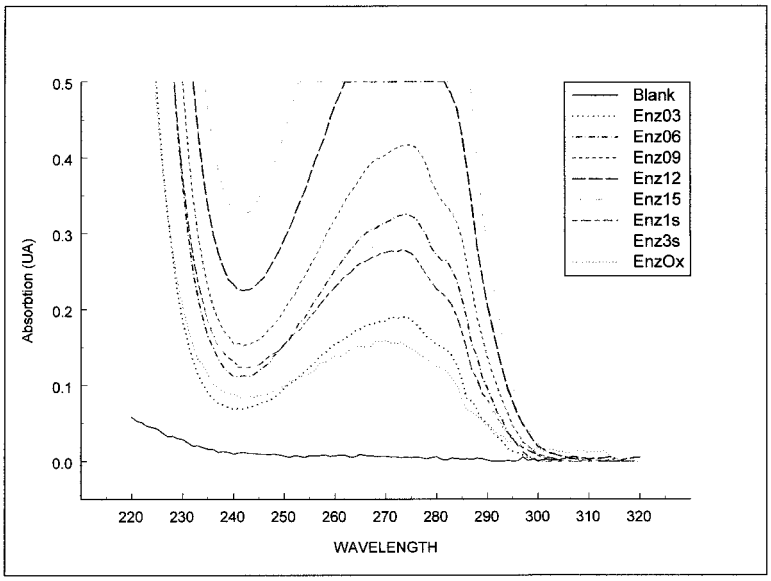

Figure 1 UV-spectra of calibration solution (3, 6, 9, 12, and 15 mg AC in 25 mL buffer) and solutions resulted after enzyme immobilization reactions (Enz1s, 1 step spacer; Enz3s, 3 steps spacer; Enz0x, enzyme directly connected to the substrate).

duced into the reactor, base pressure was created in the system, and then DS vapors were introduced, at the selected pressure and flow-rate condition, into the reactor. The plasma was ignited in the following step, and the discharge was sustained for the preselected reaction-time. At the end of the plasma reaction the reactor was evacuated to base-pressure level, followed by in situ second stage functionalization processes in the absence of plasma. During the plasma exposures the following experimental conditions were used:

- DS functionalization: base pressure, 40 mT; pressure in the absence of plasma, 200 mT; pressure in the presence of plasma, 220 mT; RF-power, 100 W; treatment time, 30 s; flow rate DS, 6 sccm.
- Oxygen functionalization: base pressure, 40 mT; pressure in the absence of plasma, 200 mT; pressure in the presence of plasma, 220 mT; RF-power, 200 W; treatment time, 60 s; flow rate O_2, 6 sccm.

Immobilization of AC was carried out according to the following procedure: plasma functionalized substrates were dipped into 25 mL of 0.02 M EPPS buffer solution. The pH of the solutions were corrected to 8.7 by adding 1 N NaOH, then 6 mg of AC was added to each solution and the solutions were kept for 45 min. Sodium cyanoborohydride (0.02 M) was then added and the films were suspended for 1 hour. At the end of the procedure the samples were washed with the buffer and then with distilled water.

One millimolar solution of 1.2 mL acetyl tyrosine ethyl ester (ATEE) and 0.15 M of 8.8 mL NaCl containing 0.5% (v/v) of Triton X-100 was used for the assay estimating the activity of the immobilized enzyme. The evaluation of pH changes during the free and immobilized AC assay has been performed by using a Virtual Instrument (LabView) serial connected to a pH-meter (Corning, Inc., Corning, NY). Data were recorded every 2 s in the interval of 0–20 min. pH-change diagrams were recorded for comparable amounts of free (1 mg) and immobilized enzyme. The enzyme uptake during the immobilization was estimated from UV absorption data at 274 nm. Calibration UV-spectra (Fig. 1) were recorded using a Varian DMS-80 instrument. The immobilized enzyme quantities were as follows: 0.88 mg, one-step spacer; 1.21 mg, three-step spacer; and 3.30 mg, direct on surface.

RESULTS AND DISCUSSION

Oxygen-Plasma-Functionalized APS and IPS Substrates

Figure 2 (A, B, and C) shows typical survey ESCA diagrams of virgin, oxygen-plasma-treated, and

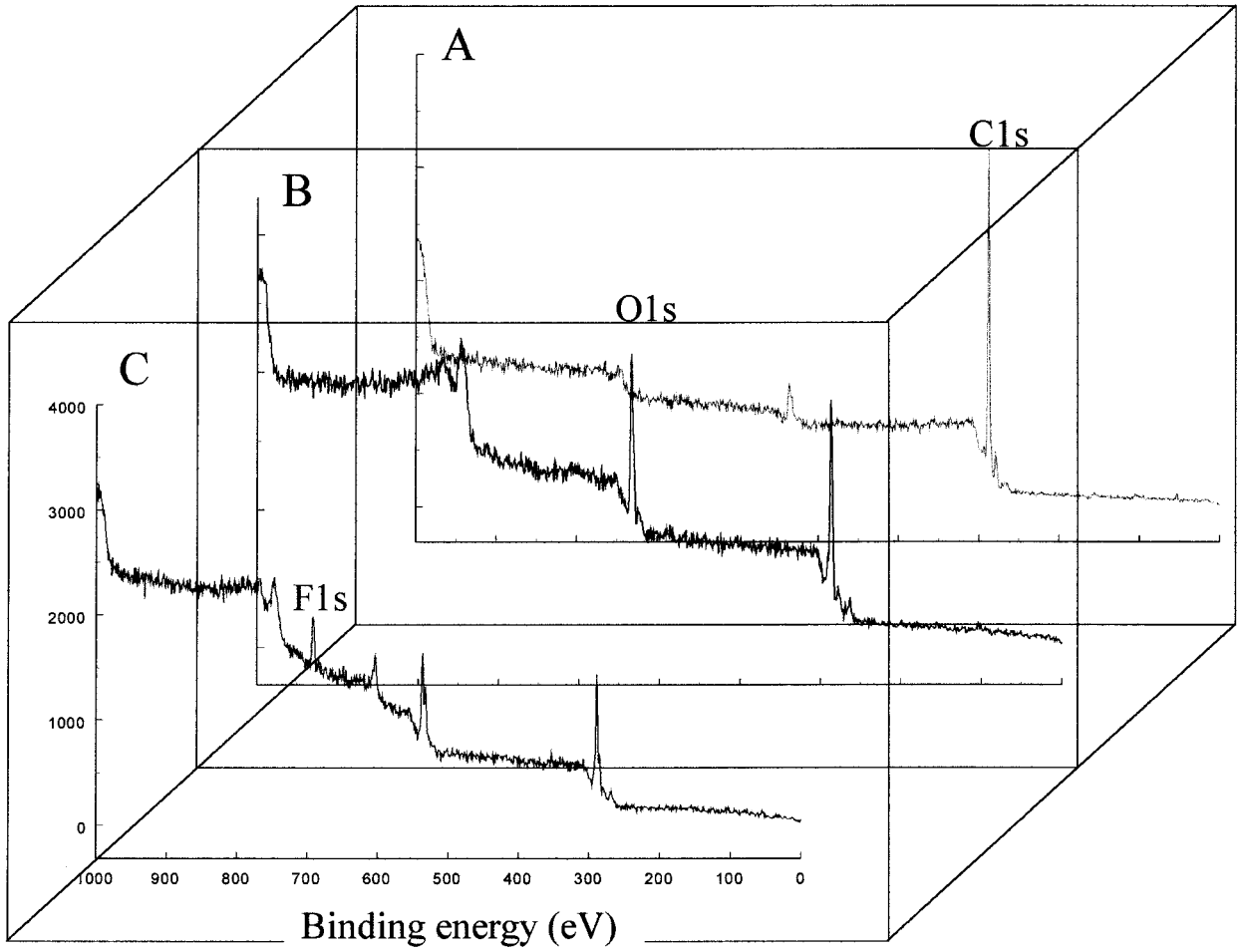

Figure 2 Survey ESCA diagrams of virgin (A), oxygen-plasma-treated (B), and oxygen-plasma-treated and PFPH-derivatized (C) IPS.

oxygen-plasma-treated and PFPH-derivatized IPS, and Figure 3 (A, B, C, and D) exhibits the comparative (survey-ESCA-origin) relative surface atomic composition of oxygen-plasma treated APS and IPS, their PFPH derivatives, and the enzyme-treated, virgin, and plasma-functionalized substrates.

It can be observed that longer oxygen-plasma-treatment times induce higher surface-oxygen and accordingly, lower carbon-atomic concentration (Fig. 3A). Relative surface oxygen-atomic concentrations as high as 39% can be achieved in 20-min plasma-treatment. It is also interesting to note that the isotactic substrate is more resistant to the plasma-generated active oxygen species; at 20 min exposure the oxygen concentrations of IPS surfaces are significantly lower (32.3%) in comparison with APS (39.9%) samples. This behavior might be explained by a selective etching of the amorphous versus the crystalline zones and by a more dense packing of macromolecules in a stereoregular structure. PFPH-derivatized, 1- and 20-min plasma-treated samples (Fig. 3B, C) show almost identical relative surface atomic compositions. This indicates that treatment times as short as 1 min are long enough for the development of efficient surface functionalization reactions. The presence of nitrogen and the fluorine atoms in the surface layers clearly indicate the existence of oxygen-plasma-created carbonyl functionalities. Relative surface atomic composition of the virgin and oxygen-plasma-treated APS and IPS with immobilized AC indicate that both atactic and isotactic plasma-exposed surfaces vigorously retain AC (5–8% nitrogen concentration). It should be noted that even the substrates that were not exposed to plasma retain minute quantities of AC (1–2% nitrogen content). It is noteworthy that significantly higher relative nitrogen-atomic concentrations are associated with

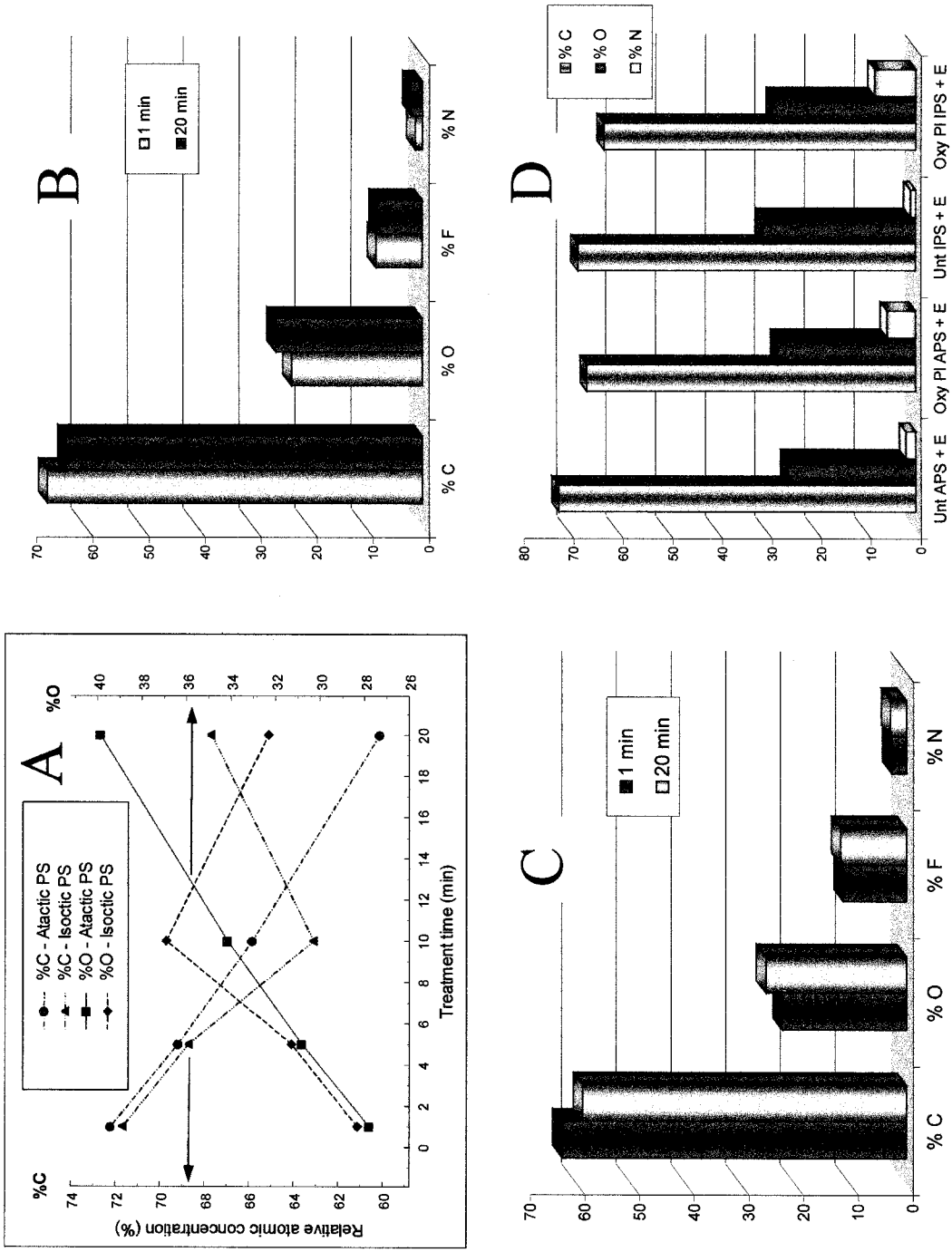

Figure 3 Comparative (survey-ESCA-origin), relative surface atomic composition of unmodified and oxygen plasma treated APS and IPS (A), PFPH derivatives of APS (B), and IPS (C), and the enzyme-treated, virgin, and plasma functionalized, substrates (D).

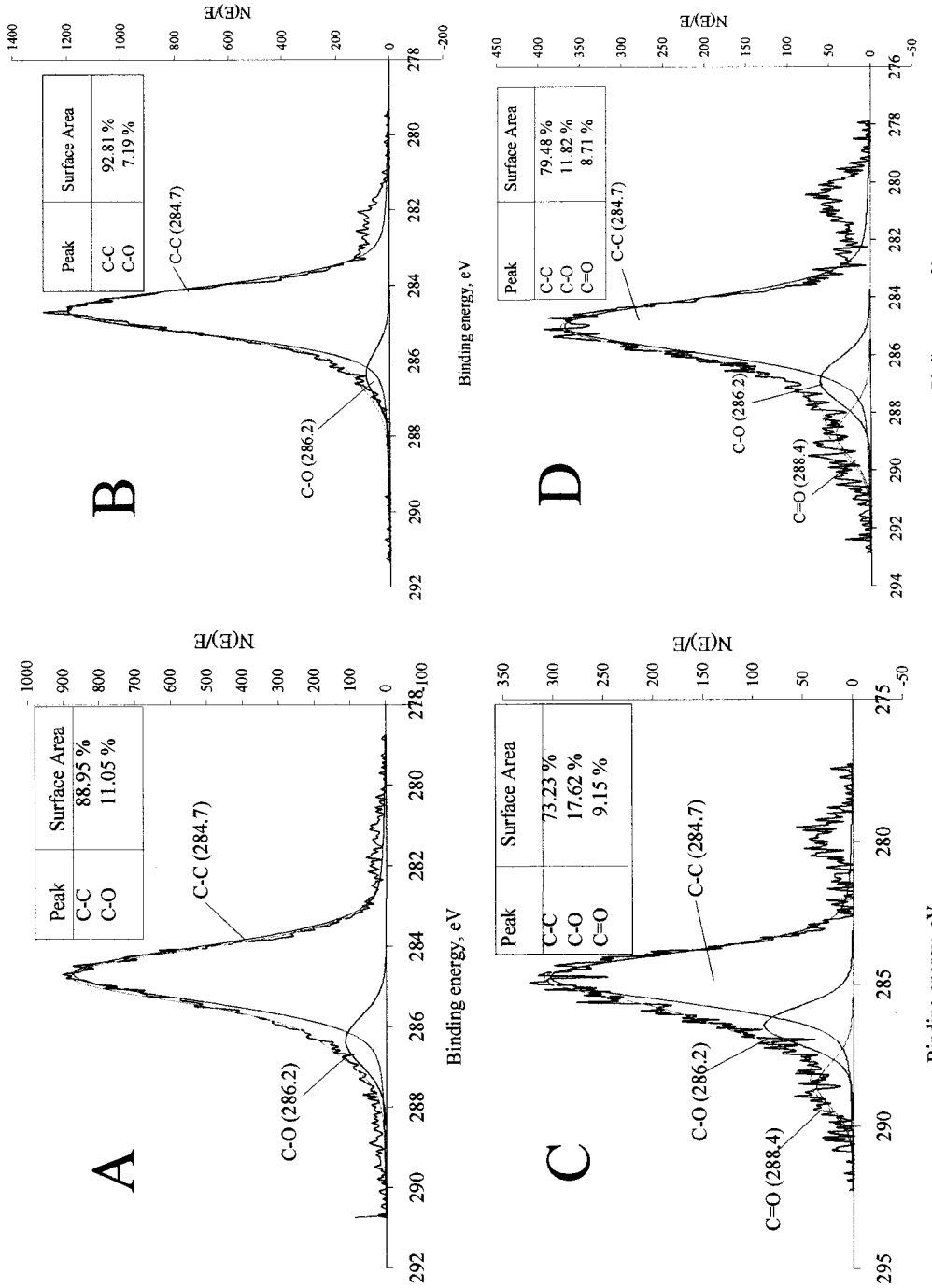

Figure 4 High-resolution ESCA data collected from virgin APS (A) and IPS (B) and from oxygen-plasma-modified APS (C) and IPS (D).

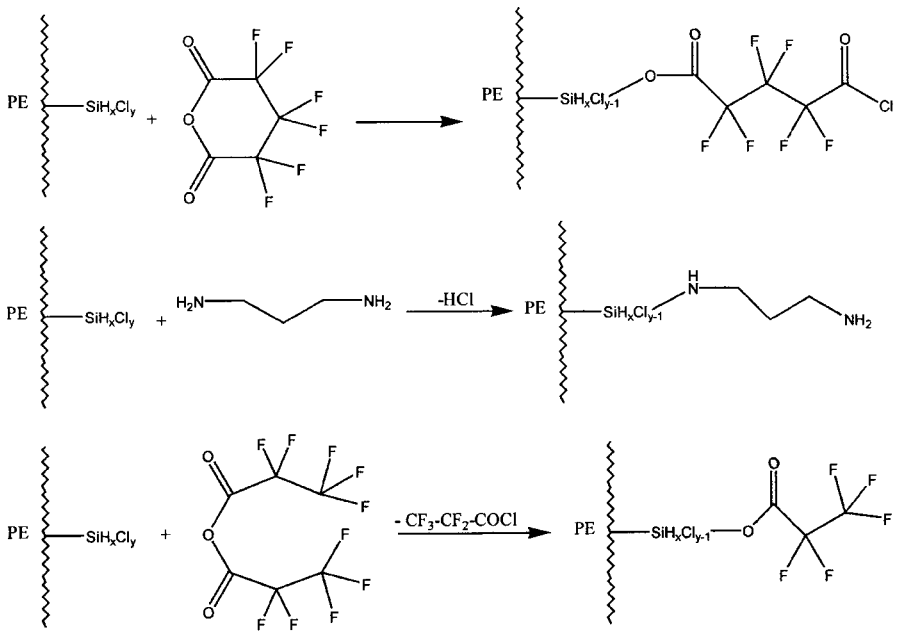

Scheme 1

IPS (8.3%) in comparison with APS (5.8%), even though the PFPH-derivatization results indicated lower C═O concentrations for the IPS substrates. This might be explained by the presence of a rougher plasma-induced, surface topography of the APS substrates, associated with a diminished availability of the functionalities for anchoring giant molecules.

High-resolution ESCA data collected from virgin and oxygen-plasma-modified APS and IPS (Fig. 4A–D), show that even unmodified PS samples have a small concentration of process-origin, C—O linkages-based (286.6 eV) oxygen content, and that the relative surface oxygen-atomic-concentration associated with IPS is lower in comparison with that of APS. Atactic and syndiotactic substrates after 20 min oxygen-plasma-exposure exhibit in addition to the C—O functionalities fairly large C═O peak (288 eV) areas. It can be noted that the relative ratios of the areas of C═O and C—O functionalities are higher in the case of IPS. This indicates a more intense carbonyl group generation on IPS (0.74) substrates relative to that of APS (0.52). However the relative surface oxygen-atomic concentration is higher in the case of APS, due probably to the less dense molecular structure.

The presence of C—F and C—N functionalities in the surface structures of the oxygen-plasma-treated and PFPH-derivatized samples could not be evaluated from the high-resolution diagrams. The low relative surface atomic concentrations of these groups, and the fact that their binding energy values (C—N: 285.8–286 eV and CF: 286–287 eV) superimpose with those of C—O linkages make deconvolution methods uncertain.

DS-Plasma-Functionalized PE Substrates

PE is an inexpensive, fairly thermally stable, lightweight (density: 0.9–0.92 g/cm^3) polymer. However, due to its high crystallinity and the absence of reactive functionalities it is chemically inert, which excludes most of the conventional wet-chemistry techniques for potential functionalization processes. Due to the comparable energy levels of cold-plasma species (electrons, ions of either polarity, free radicals, excited species, etc.) with the bond energies of most of the chemical compounds, glow discharge environments can be used to functionalize even the most inert polymeric structures under mild temperature conditions (close to room temperature).

Plasma-generated SiH_xCl_y-functionalities were implanted onto PE film surfaces and used in a subsequent step, under in situ (vacuum) conditions, for covalently anchoring spacer molecules, which expose the required functional groups at their free ends (reaction scheme A).

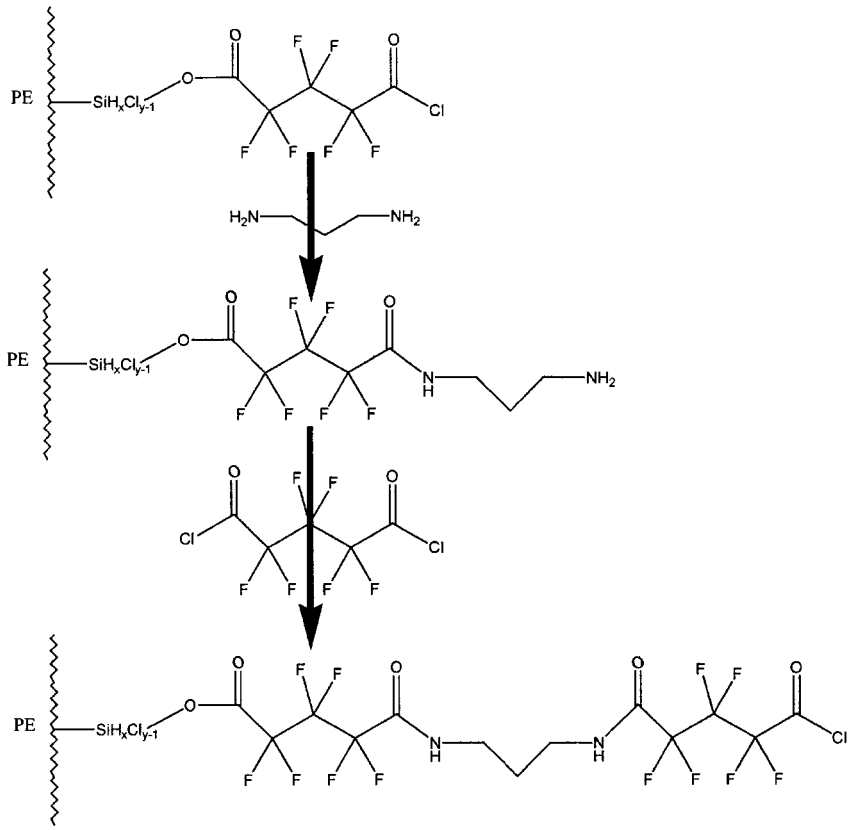

Scheme 2

These functional groups are then capable of covalently linking AC through spacer, that is, molecular chains based on various combinations of DS, HFGA, PD, HFPD, PFPA, and HFGA-PD-HFGCl molecular chains between the AC and the PE substrate (reaction scheme B).

Amides are difficult to prepare from reactions between amines and carboxylic acids. Amines generate nonelectrophilic carboxylate anions (with negative charge) and consequently they will not be attacked by nucleophiles ($RCOOH + R\text{-}NH_2 \rightarrow RCOO^- \ ^+NH_3\text{-}R$). As an alternative dichloroacids were employed instead.

The presence of covalently linked AC on PE substrate surfaces was demonstrated by comparative LD-FT/ICR/MS and differential ATR-FTIR spectroscopy. MS spectra collected from AC and intensely washed AC-immobilized PE (Fig. 5) exhibit almost identical fragmentation patterns in the 250–255 m/z region, whereas these peaks are totally absent in the spectrum of virgin PE.

Differential ATR-FTIR data collected from virgin and DS-HFGA-spacer-mediated, AC-immobilized PE (Fig. 6) confirm the presence of spacer-attached enzyme on the functionalized PE surfaces. Comparing the two specific absorption regions, at 1500–1750 cm^{-1} (which is the vibration-region characteristic for peptide linkages) and 1000–1250 cm^{-1} (vibration-zone peculiar for Si—O—Si, C—O—Si, and CF_2 functionalities), one can observe that these specific wavenumber ranges are fairly intense in the differential spectra, whereas they are totally absent in the spectra of virgin PE. The absorptions at 1664 and 1639 cm^{-1} wavenumbers were assigned to C═O absorption from secondary amides and amide I band from secondary amides. The 1066 cm^{-1} and 1209 cm^{-1} vibrations are characteristic for Si—O—Si—, Si—O—C, and CF from CF_2 groups. The narrow 1461 cm^{-1} vibration peculiar for PE (CH_2 bending) is still visible after the substraction of the spectra.

Survey ESCA-origin relative surface atomic compositions of untreated PE, DS, DS-HFGA functionalized PE, and DS-HFGA functionalized and AC-immobilized PE (Fig. 7) reflect the atomic concentration changes according to the functionalization and immobilization reactions. The relatively high nitrogen atomic concentration of the

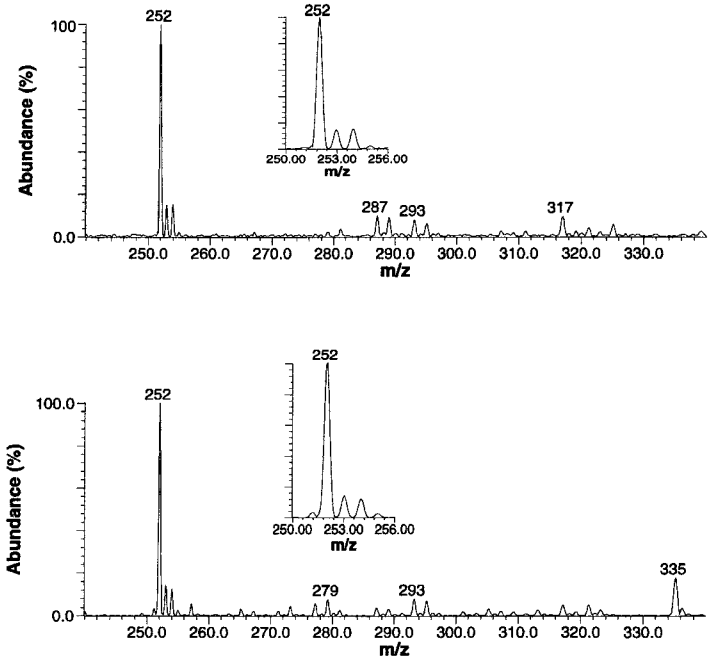

Figure 5 MS spectra collected from AC (top) and AC-immobilized PE (bottom).

AC containing surface and the high silicon and fluorine concentrations of DC-HFGA functionalized substrates indicate the development of successful derivatization and immobilization reactions.

The intercalation of spacer molecules significantly alters the surface topographies of immobilized enzymes. AFM images reveal that the hill-valley topographies of directly connected AC (C═O groups mediated covalent coupling) (Fig. 8A) is replaced by filigree (fiber-cluster-like) organizations in the case of one-step spacer-immobilized enzyme (Fig. 8B). It also can be observed that fiber-like morphologies are initiated when spacer molecules are attached to the PE surface (Figs. 8C, D, and E). It is suggested that spacer-chain-mediated, enhanced molecular freedom of motion of the enzyme allows the packing of AC

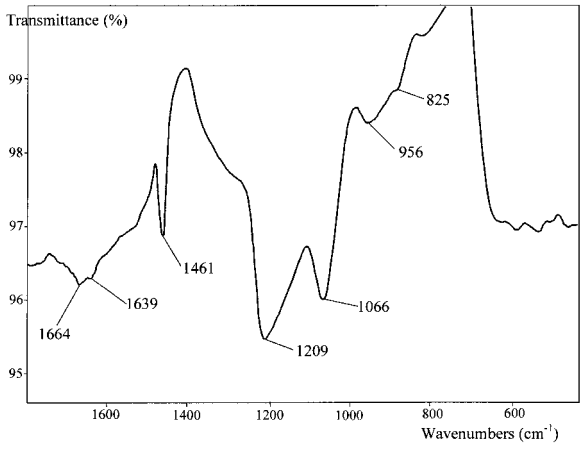

Figure 6 Differential ATR-FTIR data collected from DS-HFGA-spacer-mediated, AC-immobilized PE.

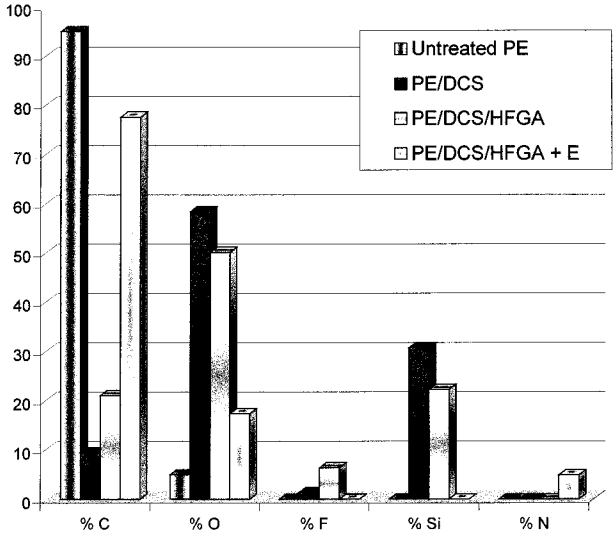

Figure 7 Survey ESCA-origin relative surface atomic compositions of untreated PE, DS, DS-HFGA functionalized PE, and DS-HFGA functionalized PE, and AC-immobilized PE.

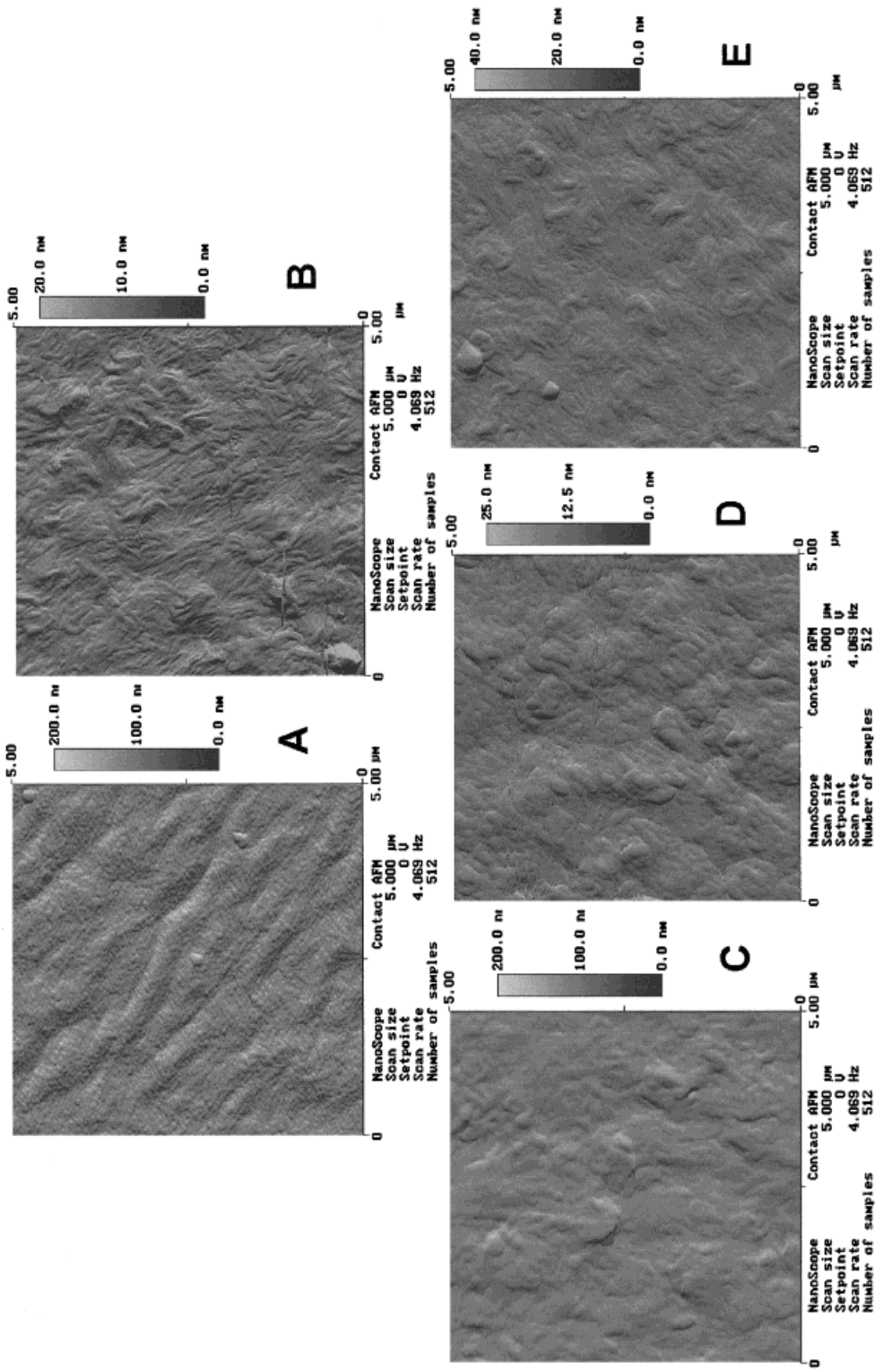

Figure 8 AFM images of: (A) AC directly attached to the PE substrate; (B) AC-immobilized involving one-step spacer; (C) virgin PE; (D) DS functionalized PE; (E) DS-HFGA functionalized PE.

Table I pH Values Measured After 5- and 20-Min Contact of the PE-Substrate Having the Immobilized AC (pH of ATEE Solution is 7.8 ± 0.1)

No.	Substrate Used	pH after 5 min	pH after 20 min
1	Free enzyme (1 mg)	5.03	4.25
2	PET and oxygen plasma[8]	7.10	6.60
3	APS and oxygen plasma	7.00	6.30
4	IPS and oxygen plasma	7.00	6.30
5	Without spacer (PE and oxygen plasma)	6.53	5.63
6	PE/DCS/PFPA	6.90	6.00
7	1-step spacer (PE/DCS/HFGA)	6.12	4.75
8	3-steps spacer (PE/DCS/HFGA/PD/HFGCl)	5.51	4.57
9	PE/DCS/HFGA/PD	7.00	5.90
10	Control experiment (without enzyme)	7.80	7.80

molecules into specific supramolecular structures.

The AC-assay test is based on the hydrolysis of the ester bond of ATEE that results in the formation of acetyl tyrosine acid. The pH of the medium will decrease with the reaction which is the measure of the activity of the immobilized enzyme. Table I presents the pH values measured after 5 and 20 min reaction of the immobilized AC with the ATEE solution.

It should be mentioned that all pH data represent average values from at least five different substrates (maximum standard deviation 0.286 and relative standard deviation 4.75%), and that the activities of immobilized systems were almost identical in ten consecutive cycles, by reusing thoroughly washed identical substrates. The only substrate was the HFGA-PD-HFGCl spacer-linked AC, which had the best activity, but the enzyme lost some of its activity (9.5%) in consecutive washing/assay cycles. This might be related to the low pH values generated during the assay that can be responsible for the deactivation of the AC.

Typical pH-change diagrams of free enzyme, one-step and three-step spacer involved, and directly attached enzyme to the PE substrate are presented on Figure 9. One can observe that the intercalation of longer spacer molecules allow the achievement of enzyme activities comparable to that of the free enzyme.

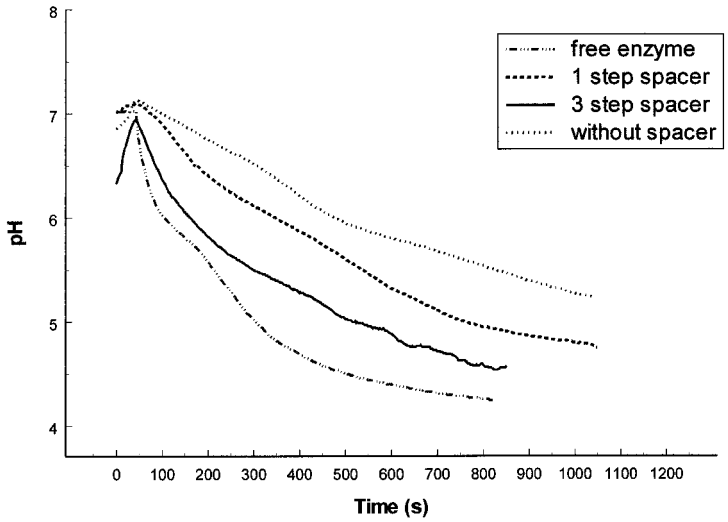

Figure 9 pH diagrams of enzyme assay involving free enzyme, one-step spacer-attached AC, three-steps spacer-attached AC, and directly attached AC to the PE substrate.

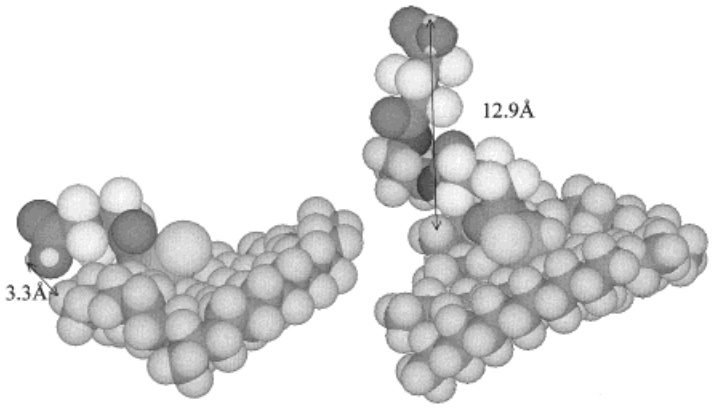

Figure 10 Space-filling models of conformation for HFGA and HFGA-PD-HFGCl spacers attached on PE surface.

The following observations can be made based on the data:

- C═O functionalized polymer surfaces allow efficient immobilization of AC regardless of the nature of the substrate, PET, PS, or PE. However, the activities of the immobilized enzymes are significantly lower in comparison with the free enzyme.
- The stereoregular nature of PS substrates does not influence the activity of immobilized AC.
- HFGA- and HFGA-HFPD-HFGCl-origin spacer molecules intercalated between the PE substrate and AC molecules distinctly improve the activity of AC.
- DS-PD spacer-molecules do not influence dramatically the activity of AC. This might be explained by the low availability (possible conformational restrictions) of enzyme-side-chain functionalities capable of reacting with primary amine groups (e.g., COOH, or C═O groups).

Conformational calculations performed on HFPD-HFGA and HGA-HFPD-HFGCl spacer chains attached to $SiCl_2H_2$-plasma functionalized PE (Fig. 10) show that the longer the spacer chain, the higher the distance (12.9 Å) between the functional chain-ends of the most probable conformational structure and the substrate. This allows us to suggest that the activity of the immobilized AC might be enhanced by the intercalation of longer spacer chain molecules as a result of increased freedom of mobility, which is in good agreement with the experimental findings.

CONCLUSIONS

AC was successfully immobilized on oxygen and $SiCl_2H_2$-RF-plasma functionalized PET, APS, IPS, and PE surfaces. It was found that the tacticity of the polystyrene substrates does not influence the activity of the immobilized enzyme.

The presence of AC on the PE substrate and the covalent nature of the anchorage was demonstrated by ESCA, ATR-FTIR, AFM, and LD-MS techniques.

It was demonstrated that longer the enzyme-anchoring spacer chain, the higher the activity of the immobilized AC. Conformational modeling correlated with the length of spacer chains allows us to suggest that the enhanced enzyme activity might be related to the freedom of mobility of AC. The stability of the immobilized AC is fairly good; it retains most of its activity after several washing/assay cycles. Many practical applications of the plasma-enhanced immobilization of enzymes can be envisaged.

It should be observed that RF-cold-plasma environments are proper for the surface functionalization even of polymeric substrates as inert as PE.

This research was funded by the National Science Foundation Grant EEC 8721545 and Hatch Federal Research Grant S-272.

REFERENCES

1. Hayashi, T.; Ikada, Y. Biotechnol Bioeng 1990, 35: 518.
2. Katchalsky, E. K. Enzyme Engineering. Weetall, H. H.; Royer, G. P.; Eds.; Plenum: New York, 1974.

3. Taylor, R. F. Protein Immobilization, Fundamental and Applications; Marcel, Dekker, Inc.: New York, 1991.
4. Yeung, E. S.; Tan, W. Anal Chem 69, 4242; 1997.
5. Lozano, P.; Manjon, A.; Romojaro, F.; Iborra, J. L. Eur Congr Biotechnol 1987, 2, 52–55.
6. Telo, J. P.; Candeias, L. P.; Empis, J. M. A.; Cabral, J. M. S.; Kennedy, J. F. Chim Oggi 1990, 8 (10), 15–18.
7. Hayashi, T.; Ikada, Y. Abstr Pap Am Chem Soc 1990, 199 Meet., Pt. 2, PMSE 113.
8. Hayashi, T.; Ikada, Y. Biotechnol Bioeng 1990, 35(5), 518.
9. Hayashi, T.; Ikada, Y. Biotechnol Bioeng 1990, 36, 593.
10. Denes, F.; Manolache, S.; Hinz, M.; Seliger, H. Immobilization of biomolecules on RF-plasma functionalized polymer surfaces; In Proceedings: 37th International Symposium on Macromolecules, Preprints; Gold Coast, Australia, July 12–17; 305; 1998.
11. Seliger, H.; Hinz, M.; Simanowski, J.; Hahner, S.; Hillenkamp, F.; Manolache, S.; Denes, F.; Gura, S.; Nitzan, B.; Margel, S.; Eisenbeiß, F. Solid-supported oligonucleotide systems for special biomedical applications, (poster 244); In Proceedings: XIII International Round Table "Nucleosides, Nucleotides and Their Biological Applications"; Montpellier, France, Sept. 6–10, 1998.
12. Denes, F.; Manolache, S. patent disclosure P99351US, 1999.
13. Ganapathy, R.; Sarmadi, M.; Denes, F. J Biomater Sci Polym Edn 1998, 9(4), 389.
14. Denes, F.; Hua, Z. Q.; Barrios, E.; Evans, J.; Young, R. A. J Macromol Sci, Pure and Appl Chem A 1995, 32(8&9), 1405.
15. Simonsick, W. J., Jr.; Ross, C. W., III. Int J Mass Spectrum Ion Process 1996, 157/158, 379.